LANDSLIDE SURFACE DEFORMATION ANALYSIS USING SBAS-INSAR IN THE SOUTHERN PART OF THE SUKABUMI AREA, INDONESIA

Muhamad Khairul ROSYIDY[1], Muhammad DIMYATI[2*], Iqbal Putut Ash SHIDIQ[3], Faris ZULKARNAIN[3], Nurul Sri RAHANINGTYAS[3], Riza Putera SYAMSUDDIN[3] and Farhan Makarim ZEIN[3]

DOI: 10.21163/GT_2021.163.11

ABSTRACT:
Landslide is a natural phenomenon that frequently occurs on the Java Island of Indonesia, causing significant damage and casualties. Due to advances in remote sensing technology, radar imaging can detect and evaluate ground surface deformation. This study examines the ground surface deformation and displacement in each landslide location in terms of spatial and temporal and identifies the different types and characteristics of landslides in the Sukabumi area of West Java, Indonesia. The Small Baseline Subset Interferometric Synthetic Aperture Radar (SBAS-InSAR) methodology was used in this study, and the DinSAR method was applied. We combined the LiCSAR data product with the Python coding-based LiCSBAS processing package to derive a surface displacement value at each landslide location. The results show that the DinSAR approach can detect surface deformation by integrating the LiCSAR product with the Python coding-based LiCSBAS processing software. According to quantitative data, the research area experienced surface deformation with a surface displacement velocity of -36,297 mm/year to 58,837 mm/year. The ground surface displacement at each landslide location ranged from -9.79 mm/year to +33.69 mm/year, with most of the landslides occurring on moderate to steep slopes (16^0-35^0). These results are suitable to use for support regional development planning in reducing losses and casualties.

Key-words: *Displacement, Deformation, Landslide, LICSBAS, SBAS-InSAR*

1. INTRODUCTION

Indonesia is prone to several different sorts of natural disasters. There were over 1,800 disasters between 2005 and 2015, with 78 percent (11,648) hydro-meteorological disasters such as floods, extreme waves, land and forest fires, drought, and extreme weather. Meanwhile, natural disasters such as earthquakes, tsunamis, volcanic eruptions, and landslides accounted for 22% (3,810 disasters) of the disasters (Amri et al., 2018). The number of disasters in Indonesia increased from 1732 in 2015 to 2342 in 2016, 2372 in 2017, and 3721 in 2019. In Indonesia, there were 702 landslides (18.9%) in 2019, resulting from 3,721 disasters (BNPB, 2019). Six hundred fifty-seven natural disasters registered in January-February 2021, with 282 fatalities, 3,421,871 people suffering and dying, and 53,287 housing being damaged (BNPB, 2021).

The surrounding area of the Sukabumi area, West Java, is one of the areas in Indonesia that frequently experiences disasters such as landslides, floods, and extreme weather (Damayanti et al.,

[1]*Departement of Geography, Faculty of Mathematics and Natural Sciences, Universitas Indonesia, 16424 Indonesia;* khairulnajwa1@gmail.com
[2*]*Faculty of Mathematics and Natural Sciences, Universitas Indonesia, 16424 Indonesia, Corresponding author,* muh.dimyati.ristekdikti@gmail.com
[3]*Faculty of Mathematics and Natural Sciences, Universitas Indonesia, 16424 Indonesia,* iqbalputut@sci.ui.ac.id, faris.zulkarnain@sci.ui.ac.id, nurul.sr@ui.ac.id,

2020). According to Alfarabi et al. (2019), the terrain, types of bedrock, and geomorphic processes can cause variations in landslides in the Sukabumi area**.** Pelabuhanratu and Cisolok areas, as a part of the Sukabumi regency, have moderate to high levels of soil movement and landslide vulnerability (Alfarabi et al., 2019; Sugianti et al., 2016). In 2018, a relatively large landslide buried 30 houses in Cisolok District, Sukabumi Regency (BNPB, 2018). This area has physical characteristics that can increase the potential of landslides (Ristya et al., 2019).

Ground movement is a geological hazard that commonly occurs in hilly areas and can result in casualties, infrastructure damage, and economic losses (Malinowska et al., 2020; North et al., 2017; Nowicki Jessee et al., 2020; Perera et al., 2018). An example of a soil movement phenomenon is landslides. Landslides are a phenomenon of the movement of soil, rocks, and organic matter down the slope due to the influence of gravity (Bobrowsky & Highland, 2013). The hydrological characteristics, geological-geotechnical conditions, slope, land use, and human activities can cause soil movement (Bogaard & Greco, 2018; Cogan & Gratchev, 2019; El Jazouli et al., 2020; Martins et al., 2020; Persichillo et al., 2017). In addition, soil movement can also be caused by human activities, such as water extraction, mining activities, cutting slopes for road construction, and others (Bateson et al., 2015; Cigna & Sowter, 2017; Hearn et al., 2020; Persichillo et al., 2017). In addition, ground movements due to landslides can cause topographic changes (Dehghani & Javadi, 2013; Guo et al., 2020). Therefore, monitoring and mapping ground movements such as landslides are necessary to minimize the risk of landslides and other ground movements (Crosetto et al., 2018; Skrzypczak et al., 2021). The value of surface deformation can be a measurable indicator for detecting landslides (Aslan et al., 2020; Qu et al., 2016; Shirani & Pasandi, 2019). The surface ground deformation can be detected using radar remote sensing, namely Synthetic Aperture Radar (SAR). SAR is also used for other applications such as measuring topographic effects by volcanic activity (Remy et al., 2003), shoreline identification (Zollini et al., 2020) and assessing ground movement by a landslide using interferometric SAR (Wasowski & Bovenga, 2014).

Interferometric SAR (InSAR) and advanced differential InSAR (A-DInSAR) are techniques that can provide centimeter to millimeter-level records of terrain topographic changes and surface deformations (Pawluszek-Filipiak & Borkowski, 2020; Ramirez et al., 2020; Roccheggiani et al., 2019). According to Ramirez et al. (2020), the DinSAR technique utilizes phase information in two or more SAR images taken at different times in the same area to form interferometric pairs. However, DinSAR has a weakness limited to signal de-correlation at the specific land cover, which interferes with interpreting deformations (Cigna & Sowter, 2017). In order to minimize the effect of de-correlation, it is necessary to use interferometric data with a short or small baseline (Pepe & Calò, 2017; Qu et al., 2016). Therefore, this study uses an advanced technique from DinSAR, namely the Small Baseline Subset Interferometric Synthetic Aperture Radar (SBAS-InSAR) approach. According to Bateson et al. (2015), this approach consists of many SAR data acquisitions spread over a small subset of baselines**.** SBAS-InSAR approach allows for an effortless combination of computationally calculated InSAR data and standard processing techniques based on deformation time sequences (Bateson et al., 2015). This approach relies on using a large number of SAR data acquisitions and applying an effortless combination of a selected and computed set of multi-look DinSAR interferograms so that the result is a time-series map of the mean velocity of deformation and ground motion (Casu et al., 2006; De Luca et al., 2018; Yastika et al., 2019). According to Bateson et al. (2015), SBAS is suitable to detect land surface deformation in rural areas. To carry out this technique, LiCSBAS is used to process SAR data. LiCSBAS is a LiCSAR product data processing package developed by Morishita et al. (2020) to process time-series InSAR and estimate deformation velocity. LiCSAR is a collection of free-access interferogram data of Sentinel-1 imageries from the COMET-LiCS portal (Morishita et al. 2020). Sentinel-1 imagery data can be used for various geotechnical engineering phenomena because it has a C band, a 10-meter resolution, and free-open access with worldwide coverage (Ramirez et al., 2020). Other researchers have not widely used LiCSAR products and LiCSBAS processing packages because they are relatively new and are still under development by Morishita et al.

Several researchers have studied and researched using the SBAS-DinSAR technique and have proven to be better for producing deformation maps than conventional DinSAR techniques. For example, Lanari et al. (2007) used the SBAS-InSAR method for the phenomenon of fault creep using 45 ERS-1/2 images. As a result, they succeeded in calculating the relative soil movement along the fault with better accuracy of 1 mm/year than field deformation measurements. SBAS can also detect ground motion due to human activities such as mining and groundwater extraction. For example, Bateson et al. (2015) utilized 55 ERS-1/2 SAR images for the 1992-1999 period to detect movements in coal mining areas in the UK using the SBAS method.

Regarding landslides, Qu et al. (2016) used the SBAS method to detect soil movement in the landslide area extracted from TerraSAR data for 2014-2015. (Novellino et al. 2017) that as many as 266 landslides with low-velocity movement (shallow landslides) were detected using the SBAS-DinSAR method. According to Novellino et al. (2017), the SBAS- DinSAR method can generate relevant information to detect slow soil movements such as slides, flows, and creep movements that dominate the evolution of slope geomorphology. Cianflone et al. (2018) conducted a mapping of landslides and land surface deformations in 2004-2010 in the Crati valley (southern Italy) using the SBAS-InSAR technique. The results showed the most soil movements detected by mass movements InSAR gravity, such as landslides and a decrease in the quaternary sediment that fills the valley.

The SBAS-InSAR technique, combined with the LICSAR and LICBAS processing packages, is still not widely utilized to assess surface ground deformation, as indicated by the references above. Meanwhile, the dynamics of landslides in Indonesia, particularly in steep and difficult-to-reach areas and densely populated areas, are being explored. Areas with an increased risk of landslides, such as Sukabumi, have missed the attention of previous researchers in this assessment. Access to radar images, on the other hand, is improving. As a result, we intend to research using radar imagery to analyze surface ground deformation in Sukabumi**.** This study uses the Small Baseline Subset Interferometric Synthetic Aperture Radar (SBAS-InSAR) technique by combining the LICSAR product and the LICSBAS Package**.** The last is conducting field surveys and documentation as the basis for determining the location of landslides**.**

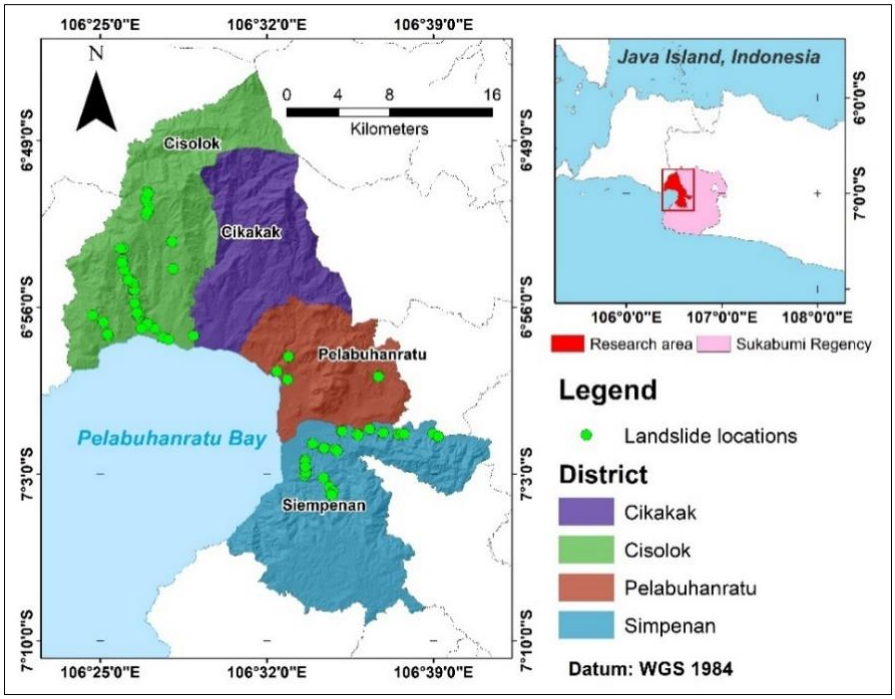

Fig. 1. Study area and Landslide location.

2. STUDY AREA

The study area is in the southern part of the Sukabumi area, includes Pelabuhanratu, Simpenan, Cisolok, and Cikakak Districts of Sukabumi area, West Java Province, Indonesia (**Fig. 1**). The study area is geographically located at 6°46'4 " S latitude - 7°9'25 " S latitude and 106°23'22 " E longitude - 106°41'27 " E longitude whole study area has a total area of 55,038 ha. The slopes in the study area range from modest to quite steep. The volcanic material associated with Quaternary volcanic eruptions such as breccias, lava, lahars, and tuff dominates the Sukabumi Regency area. Predominantly, the southern part of Sukabumi consists of an accumulation of alluvium deposits and coastal sediment deposits (Sugianti et al., 2016). Soil types in the study area consist of alluvial sulfic, andosol, cambisol, cambisol eutric, and podsolic haplic (Alfarabi et al., 2019). The study area has a medium to a high level of landslide susceptibility, which is impacted by physical factors of the location (geology, soil type, rainfall, land use, and geomorphology). Those factors increase the possibility for soil movements such as landslides (Alfarabi et al., 2019; Ristya et al., 2019; Sugianti et al., 2016). Based on Indonesian disaster information data obtained from https://dibi.bnpb.go.id/, 90 Landslides disasters occurred in the Sukabumi Regency from 2017 to 2020.

3. DATA AND METHODS

3.1. LiCSAR Dataset

The images utilized in this study are processed data from Sentinel-1A IW SLC images with VV polarization that were processed and downloaded to the COMET-Lics (Center for the Observation and Modeling of Earthquake Volcanoes and Tectonics) online portal named LiCSAR (comet.nerc.ac.uk). Processing sentinel-1 imageries data through the stages of correlation, spectral diversity correction, unwrapping, and multi-look to produce time-series coherence, and unwarp phase data in the form of an interferogram with pixel size or spatial resolution of 100 meters in the LiCSAR product (Morishita et al., 2020). LiCSAR time-series Sentinel-1 data with ascending satellite records from April 9, 2019 to August 13, 2020 was used in this study. **Fig. 2** illustrates the perpendicular baseline network. The basis for selecting the acquisition period is that the imageries have a low temporal baseline, resulting in low noise in the interferogram data. Sentinel-1a single look complex (SLC) imagery wide swath mode (IW) with VV polarization, ascending satellite recording direction, and LiCSAR frame id 047D 09652 111009 were the image data parameters used in this study. There are 107 interferograms in total.

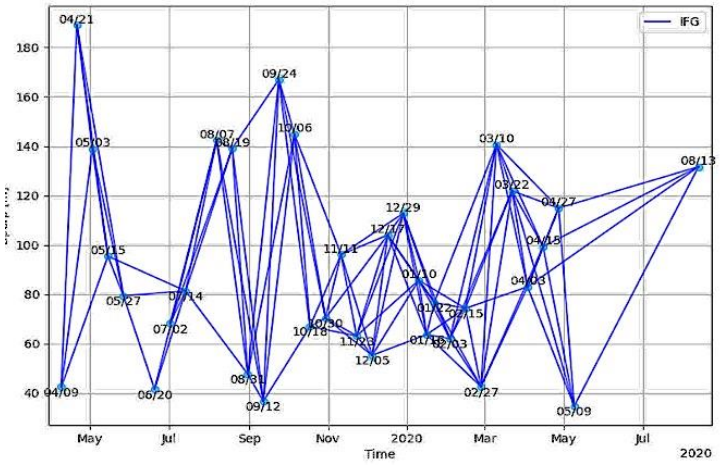

Fig. 2. Temporal baseline network of 107 interferograms constructed from 33 Sentinel-1 Imageries.

3.2. SBAS-InSAR Method using LiCSBAS Processing Package

The Small Baseline Subset (SBAS) approach analyzes LiCSAR data through LiCSBAS on the Linux Ubuntu 20.04 LT operating system. Berardino et al. (2002) developed SBAS, an advanced processing approach for the DinSAR (Differential Interferometric Synthetic Aperture Radar) methodology (Berardino et al., 2002). The goal of this method is to measure multi-temporal ground motion and map the average deformation velocity with an accuracy of up to millimeters by combining unwrapped interferograms by spatially isolating them from the baseline between each orbital acquisition at short intervals (Berardino et al., 2002; De Luca et al., 2018). The essence of this approach is the improvement of the inversion of unwrapped interferograms for time-series deformation (Lanari et al., 2007). In addition, the SBAS processing produces a soil movement map with a precision of mm/year. In this study, the SBAS method processing runs using LicSBAS, which is a LicSAR data processing tool based on Python 3 coding, and Bourne Again Shell (bash), which operates without using software (open source) (Morishita et al., 2020). According to Morishita et al. (2020), LiCSBAS lets users interpret InSAR data in time series and estimate soil movement velocity using LiCSAR products available on the COMET-Lics.

Figure 3 shows a research workflow that illustrates the detailed analysis process. Data preparation from a series of unwrapped images and multi-temporal analysis are the two critical processes of LiCSBAS's InSAR processing. First, data preparation comprises downloading LiCSAR data from the COMET-Lics web page in the form of unwrapped and coherent GeoTIFF files (comet.nerc.ac.uk). The data comes from Sentinel-1 frame ID image 047D 09652 111009, acquired for 1.35 years, from April 9, 2019, to August 13, 2020. The following stages converge GeoTIFF into a single-specification point format and use GACOS to correct atmospheric disturbances on the unwrapped interferogram (Generic Atmospheric Correction Online Service). Masking and clipping the interferogram to remove areas with less than 0.5 coherence and cutting the research area with coordinates ("106°19'48 N / 107°4'58,8 S / 7°27'14,2 W / 6°42'3,6 E") and a square area of interest are the final steps in data preparation.

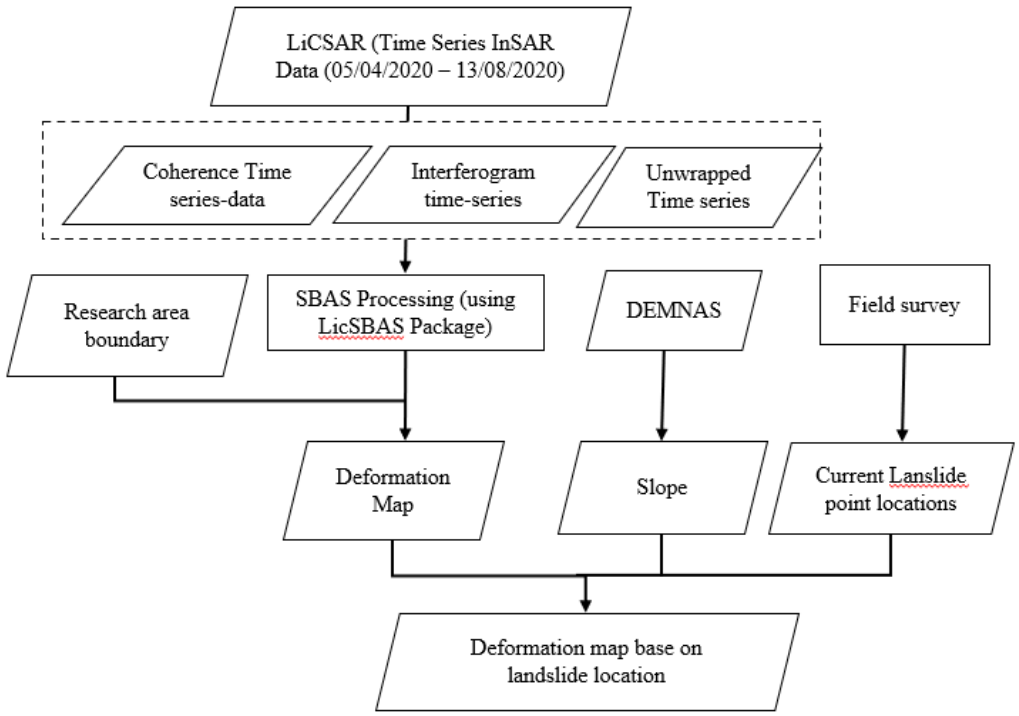

Fig 3. Research Workflow.

The multi-temporal analysis step is divided into multiple stages, beginning with a quality check of the LiCSAR interferogram result by determining the coherence average to eliminate the impacts of de-correlation caused by vegetation or other factors. The next step is to use a closed-loop to repair the network by removing unwrapping errors. The next step is the inversion of the small baseline network, which calculates the pixel surface's vertical and horizontal movement velocity from April 9, 2019, to August 13, 2020. The final steps determine the standard velocity deviation, masking of noisy pixels, and spatial-temporal filtering. The results are Line-of-Sight Displacement or LoS Displacement, which is an indicator of ground surface movement velocity. The LoS value is the result of measuring the movement of the surface at a place on the earth's surface estimated by the SAR antenna, according to Li et al. (2019). The LoS Displacement value is assumed to directly reflect vertical movement or elevation changes (Ng et al., 2012).

The landslide locations of the southern part of the Sukabumi area, which includes Pelabuhanratu, Simpenan, Cisolok, and Cikakak District, are overlaid with the deformation map derived using the SBAS method. The overlay intends to use a spatially descriptive approach to assess the deformation that occurs at landslide locations.

To analyze the landslide point elevation and deformation value, we overlay the 8-meter resolution DEMNAS obtained from the Geospatial Information Agency webpage at http://tides.big.go.id/ over the landslide locations. On November 21-25, 2020, eighty-nine landslide point locations were collected using survey and field documentation.

4. RESULTS AND DISCUSSIONS

4.1. Spatial Distribution of Surface Deformation

The results of InSAR processing using the SBAS method from LiCSAR data suggest that the study area has a relatively coherence value. The coherence value has a minimum of 0.032 and a high of 0.834 in the research area. The coherence value indicates how accurate InSAR processing is (**Fig. 4**). The closer the InSAR processing results are to 1, the more accurate they will be. A high coherence value means that the entering backscatter signal is nearly identical to the reflected backscatter signal, allowing the reflected signal to maintain its amplitude without considerable change. The incoming signal collides with a stationary or immovable object, such as built-up or bare land. Because it is a port area and many built-up areas, the coastline region in the study area has a high coherence value. Environments with poor coherence values, on the other hand, are found in densely vegetated areas such as forests. Because radar wave emission does not fully represent the deformation process in low coherence locations, areas with low coherence are not always deformed. Increased noise levels in the InSAR phase measurement are related to reduced coherence values in the interferogram (Anjasmara et al., 2020).

According to data processing, from April 9, 2019 to August 13, 2020, the rate of change in land elevation ranges from -36,297 mm/year to 58,837 mm/year (**Fig. 5**). Negative rate values imply land surface subsidence, whereas positive rate values indicate land surface increase (uplift). In the research area, negative results for the rate of change in height can be seen in coastal and hilly locations.

Land subsidence ranging from 10 mm/year to 5 mm/year has been seen in the coastal areas of Pelabuhanratu in the south and the North Coastal Area in Simpenan District. Positive displacement values are seen in most coastal locations in the research area, particularly in flat and intensively built-up areas. In the area along the coast, the displacement velocity is typically negative. In the area near the coast, displacement values range from less than -10 mm/year to more than +10 mm/year.

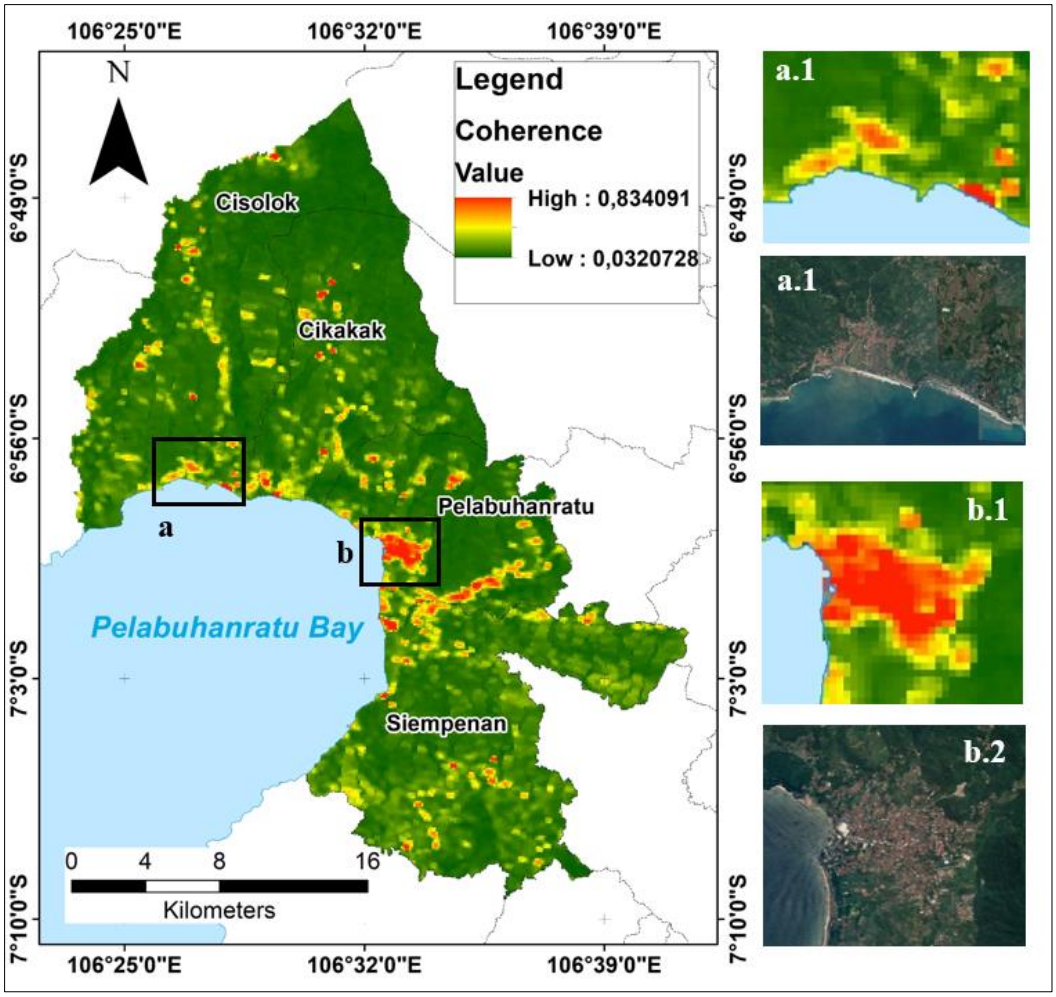

Fig.4. Coherence Map in Research Area. **4.a.1** and **4.a.2** show the built-up land with a high level of coherence in the Coastal area of Cisolok District. **4.b.1** and **4.b.2** shows built-up land with a high level of coherence in the Coastal of Pelabuhanratu District**.**

According to data analysis, the uplift area is larger than the sinking area. The area affected by subsidence was 1,623 hectares (2.9%), while the area affected by uplift was 8,275 hectares (15.0 %). Subsidence is most common in locations where the slopes are gentle to slightly steep. As a result, there are cracks in the buildings and a substantial change in ground level in the surrounding area experiencing subsidence. Fields that experience an uplift are usually development or land accumulation near rivers and valleys. According to the field study, there is development along the coast, particularly in the coastal area of the Pelabuhanratu District.

4.2. Surface Displacement in Each Landslide Locations

The landslide locations were collected as part of a field survey in November 2020, with several of the 89 points being landslide/soil movement locations. The major landslides found in the study area are Translation landslides, rockfalls, and spreads (**Fig. 6)**.

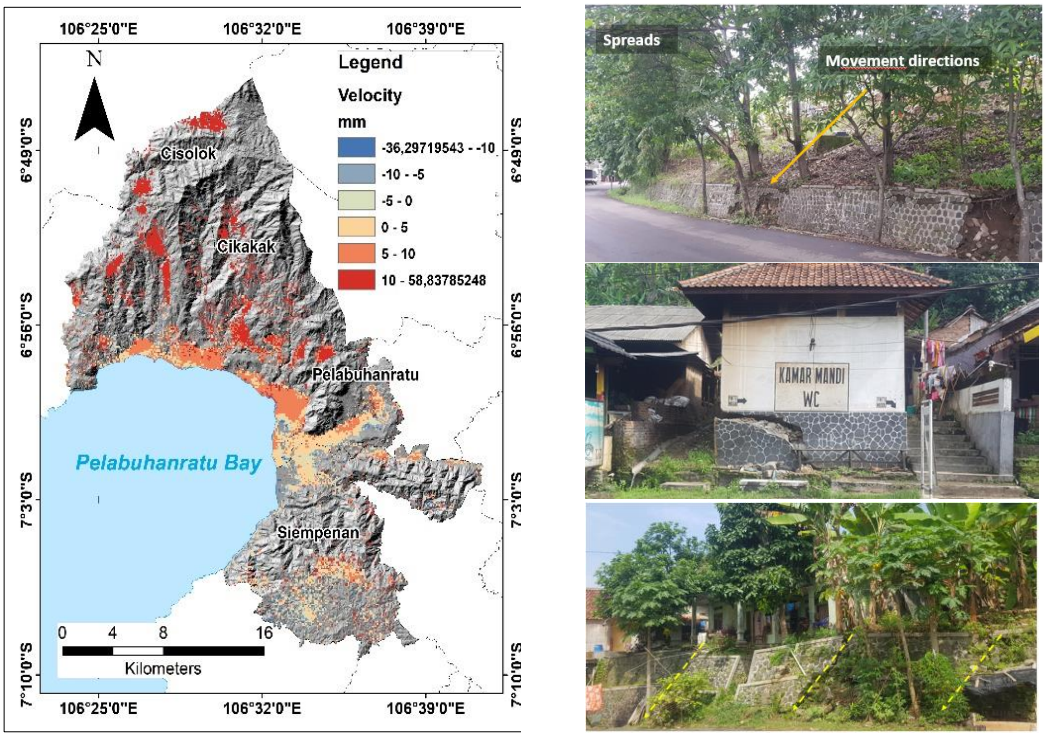

(a) **(b)**

Fig. 5. (5.a) Spatial distribution of Surface Deformation in Pelabuhanratu District, (5.b) Subsidence in Research Area.

In the research area, translational landslides occur in mountainous areas with steep to steep slopes, causing the soil mass movement to slide down the slope (Bobrowsky & Highland, 2013)**.** In the translational landslides, scrub vegetation dominated the land cover. The translation landslides found in the field survey are primarily shallow, 4 to 8 meters deep. Cisolok and Simpenan districts are prone to translational landslides. Rockfalls were found in the south part of the study area (Simpenan District). In general, rockfalls are found predominantly in cliff locations and along roads (**Fig. 6)**. The vegetation is relatively dense and dominated by dense vegetation because the surrounding area is a forest. Spreads are generally slow-moving (Bobrowsky & Highland, 2013). This landslide was recognized by the cracks between the road and houses, resulting in differences in height (**Fig. 5.b)**. Soil sediment can occur due to mechanical processes on slopes, pedo-genetic, and bio-geomorphic activity, and it can also be influenced by deformed tree cover in forest environments (Pawlik & Šamonil, 2018).

Landslide locations are analyzed based on the degree of slope, slope characteristics, and their relationship to landslides (**Fig 7**). According to (Berhane et al., 2020), slope angle can be related to landslides because slopes can determine surface and subsurface flow direction and significantly impact soil moisture availability, which affects slope stability. The classification of slopes is based on Zuidam et al. (1985) (Zuidam, 1985). The 89 collected landslide locations with a slope of (16^0-35^0) have the highest frequency of deformation, indicating a relatively steep slope. The highest frequency of subsidence was found at a landslide location on a very steep slope (16^0-35^0), where 22 landslide locations were identified.

Fig. 6. landslides found in the study area.

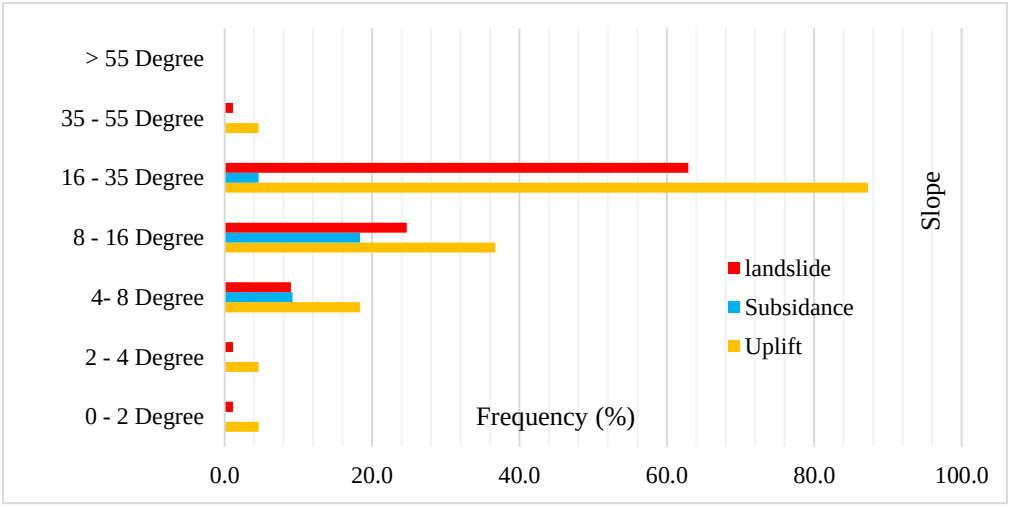

Fig. 7. Landslide frequency in each slope and deformation frequency in each slope based on landslide location.

Thus, there were 22 landslides, with the highest frequency occurring at landslide locations with varied slopes, from moderate to steep slopes (16^0-35^0). Because erosion is frequent and soil movement is gradual, landslides are more likely to occur on slopes of (16^0-35^0) and less than 15 (Çellek, 2020). Furthermore, landslides are rare on slopes with a slope angle greater than 35^0 since the bedrock has been exposed to erosion. This condition is because the slope vulnerability is inversely proportional to the angle value on the slope since it increases the soil shear stress (Çellek, 2020).

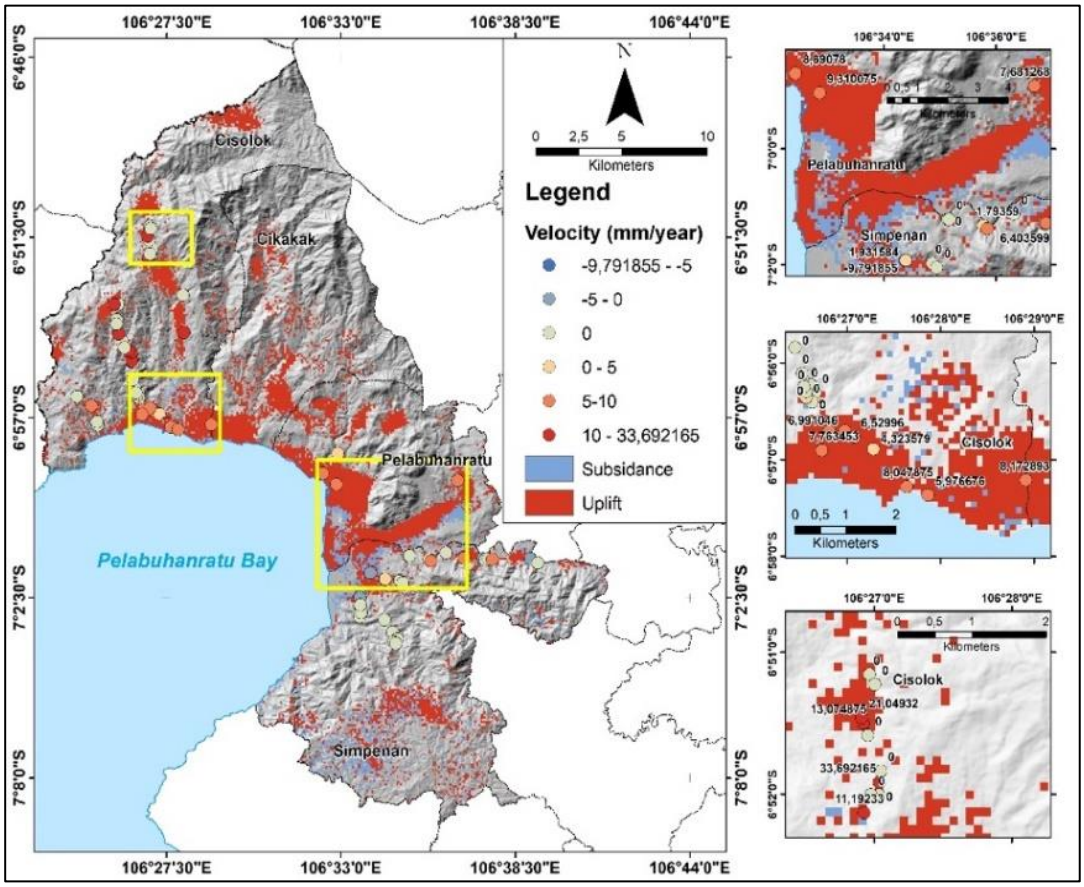

Fig. 8. Deformation value distribution in landslide point locations.

The landslide location is used to extract the displacement value acquired through LiCSBAS processing, resulting in a landslide location distribution map based on the displacement value (**Fig. 8**). Seven landslide locations in the study area experienced subsidence, whereas 33 landslide locations experienced uplift, according to the results of the deformation map overlay and landslide locations in the study area. The remaining are landslide locations that are not detected by satellite signals because vegetation cover interfering with satellite signals or processing errors in InSAR data. Each landslide location's deformation velocity was divided into six categories. The landslide's displacement velocity varies from -9.79 mm/year to +33.69 mm/year at each point. There is one landslide location in the Pelabuhanratu and Simpenan Districts with a displacement velocity of less than 5 mm/year, a minimum velocity of 9.79 mm/year, and a maximum velocity of 4.54 mm/year. There are four landslide locations with displacement velocities ranging from -5 mm/year to 0 mm/year. The most negligible displacement velocity is 4.54 millimeters per year, while the maximum velocity is 0.068 millimeters per year. The Cisolok and Simpenan Districts were the sites to the majority of the landslide locations that experienced negative displacement. The negative value at the landslide location is assumed to be a depletion zone, while the positive value is assumed to be an accumulation zone. Because the distance between a location on the earth's surface and the radar satellite sensor is far from each other, the depletion zone has a negative displacement value. The displacement value is positive because the point on the earth's surface approaches the radar satellite sensor (Aslan et al., 2020).

Positive displacement landslide areas have a minimum velocity of 1.79 mm. Favorable displacement velocity locations with a minimum velocity of 1.79 mm/year and a maximum velocity of 33.69 mm/year are found in 33 locations in the Cisolok, Cikakak, Pelabuhanratu, and Simpenan Districts. In the Cisolok District, the landslide location with the highest positive displacement value is 33.69 mm/year. There are ten landslide locations with displacement values of more than 10 millimeters per year. The displacement velocities of 16 landslide areas range from 5 mm/year to 10 mm/year. Positive displacement values of less than 5 mm/year are found in seven landslide locations. Forty-nine landslide locations had displacement with a value of 0. The SBAS-DinSAR technique does not detect the landslide location since DinSAR's ability is limited to locations with minor de-correlation and errors. Furthermore, development in the Pelabuhanratu coastline area has an impact on the displacement value.

5. DISCUSSIONS

The displacement value was obtained from 107 interferograms resulted from 33 Sentinel-1 images recorded from April 9, 2019 to August 13, 2020. The Sentinel-1 image interferogram obtained from the COMET-Lics web portal was used to process LiCSBAS. The displacement value obtained from the SBAS-DinSAR processing is -36.29 mm/year to 58.83 mm/year. This study shows that most of the displacements with positive values (uplift) are in residential areas, in coastal areas, and several locations in hilly areas, such as in Cisolok, Pelabuhan Ratu, and Cikakak districts. Meanwhile, the negative displacement value (subsidence) is located on the coast of Simpenan District, dominated by hills. With the same method, Anjasmara et al. (2020) produced displacement values in the City of Surabaya in a range of -40 mm/year to +30 mm/year using 28 Sentinel-1 images recorded from 2015-2017 (Anjasmara et al., 2020). Most of the subsidence occurs in industrial and residential areas in the coastal area of Surabaya City. Virk et al. (2019) used the same imagery dataset and 23 descending Sentinel-1 images and the PS-InSAR approach to monitoring ground displacement on landslide locations (Virk et al., 2019).

In addition, Zaenudin et al. (2018) used data from 15 ALOS PALSAR images recorded between 2006 and 2008 to derive a subsidence value of more than 30 mm/year in Bandar Lampung City. The coastline area of Bandar Lampung City has a subsidence value of more than 5 mm/year, according to Zaenudin et al. (2018). Ng et al. (2012) employed another InSAR approach, the PS-InSAR, to map land surface deformation in the Jakarta area and its surrounds using 17 ALOS PALSAR (band L) images acquired between 2007 and 2010. A survey including GPS measurements was used to round out the results of the study. In the northern part of Jakarta, the subsidence value reached 260 mm/year, with the Bekasi metropolitan region having the highest subsidence value of 155 mm/year. Prasetyo et al. (2019) used Sentinel-1 imagery data from 2014 to 2017 to study land subsidence in Semarang City using the PS-InSAR technique. The measured displacement ranges from -4.4 cm/year (-44 mm/year) to -3.4 cm/year (34 mm/year). According to the research, the displacement value produced above is generally higher than 30 mm/year.

Land cover/use is the most common factor influencing the displacement value (Anjasmara et al., 2020). The type of land cover/land use significantly impacts the data's accuracy (Castellazzi & Schmid, 2021; Zaenudin et al., 2018). The land cover/land use type significantly impacts the data's accuracy (Castellazzi & Schmid, 2021; Zaenudin et al., 2018). The information on deformation velocity obtained by the InSAR-SBAS approach gets less accurate as the area becomes more dynamic than usual. The quality of the deformation information generated is not appropriate for measuring deformations with one-millimeter accuracy.

This research provided use of the LiCSAR dataset and the LiCSBAS processing package, which was recently developed by Morishita et al. (2020) and claimed to minimize processing time efficiency and demonstrate promising results in describing deformation in a relatively large area that has not been widely used. The difference between this study and Morishita's research is that this study was conducted in the Sukabumi area. In order to minimize the contribution of noise reduction and the detailing of deformation values, this study uses different characteristics of temporal data.

We also look at the deformation at each landslide location and evaluate it according to the slope. Because of the differences in the characteristics and environment of the research area, this was done. The study demonstrates that at the Sukabumi area, the accuracy of displacement and deformation data is relatively good. Therefore, the result of the study is consistent with Morishita's findings.

The types of land cover in the research area impact the accuracy of this study's displacement and deformation measurements (Zaenudin et al., 2018; Anjasmara et al., 2020; Castellazzi & Schmid, 2021). The vegetation land cover dominates the southern part of the Sukabumi area. The density of vegetation might affect the coherence value and contribute noise to the processing results. As a result, the study's surface deformation is shown in areas with little vegetation, such as villages and bare land. The more dynamic an object is on the earth's surface, the detected deformation and displacement value information get less accurate for measuring deformation with millimeter accuracy (Zaenudin et al., 2018).

6. CONCLUSIONS

The ground surface deformation at each landslide location in the Sukabumi area was studied and mapped using the InSAR method using the SBAS approach. The surface deformation was processed using a python coding-based LiCSAR dataset and the LiCSBAS processing package, recently developed by Morishita et al. (2020). These products and packages might detect ground surface deformation in landslides as radar images become more accessible because they are not widely used to analyze ground surface deformation. Those methods were reported to have an mm/year precision and the ability to reduce processing time and produce good results in describing deformation in a relatively large area that had not ever been studied. Pixels with a dimension of 100 meters x 100 meters reflect the rate of change in ground surface elevation. Morishita's research differs from ours because of the diverse locations and environment and temporal radar data, the evaluation of deformation at each landslide location, and slope evaluation. For the Sukabumi area, we use LiCSAR product data, which is Sentinel-1 image data already in the form of unwrapped interferograms, recorded from April 9, 2019, to August 13, 2020. The processing findings using the SBAS approach demonstrate that the Pelabuhanratu area and its surroundings experienced land surface deformation from April 2019 to August 2020, with rates of change in elevation ranging from -36,297 mm/year to 58,837 mm/year. The area affected by subsidence was 1,623 hectares (2.9 percent), while the area affected by uplift was 8,275 hectares (15.0 percent). The rest was an area where surface deformation was not identified.

At each landslide location documented in the field, we also measured the rate of ground surface deformation. The displacement rate at each landslide location ranges from -9.79 mm/year to +33.69 mm/year, based on data LiCSBAS processing using the SBAS method. Uplift was observed in 37.1 percent of landslide locations (Pelabuhanratu, Simpenan, Cikakak, and Cisolok Districts), while subsidence was detected in 7.9 percent (Simpenan and Cisolok Districts). The positive displacement value at the landslide location is assumed to be the landslide's accumulation point. The landslide locations found in the field are often shallow landslides with a depth of fewer than 10 meters, with a typology of translation landslides, spreads, and rockfalls.

The most significant frequency of landslide locations and their movements (subsidence and uplift) found in the field are on moderately sloping to steep slopes, according to the results of the landslide location analysis of the physicochemical properties of slopes in the study area (16^0-35^0). The detection of surface deformation and displacement at each landslide location in the southern Sukabumi area was successfully demonstrated in this study. The findings are consistent with Morishiuta’s study findings.

ACKNOWLEDGEMENTS

We are grateful to the Ministry of Research and Technology/National Research and Innovation Agency for support and research funding through Insinas (National Innovation System Incentive). We also thank members of the Department of Geography, Universitas Indonesia, for their encouragement.

REFERENCES

Alfarabi, M. S., Supriatna, Manessa, M. D. M., Rustanto, A., & Ristya, Y. (2019). Geomorphology and Landslide-Prone Area in Cisolok District, Sukabumi Regency. *E3S Web of Conferences*, *125*(201 9), 1–6. https://doi.org/10.1051/e3sconf/201912501005

Amri, M. R., Yulianti, G., Yunus, R., Wiguna, S., W. Adi, A., Ichwana, A. N., & Randongkir, Roling Evans Septian, R. T. (2018). RBI (Risiko Bencana Indonesia). In *BNPB Direktorat Pengurangan Risiko Bencana* (Vol. 9, Issue 3).

Anjasmara, I. M., Yulyta, S. A., & Taufik, M. (2020). Application of time series InSAR (SBAS) method using Sentinel-1A data for land subsidence detection in Surabaya city. *International Journal on Advanced Science, Engineering and Information Technology*, *10*(1), 191–197. https://doi.org/10.18517/ijaseit.10.1.6749

Aslan, G., Foumelis, M., Raucoules, D., De Michele, M., Bernardie, S., & Cakir, Z. (2020). Landslide mapping and monitoring using persistent scatterer interferometry (PSI) technique in the French Alps. *Remote Sensing*, *12*(8). https://doi.org/10.3390/RS12081305

Bateson, L., Cigna, F., Boon, D., & Sowter, A. (2015). The application of the intermittent SBAS (ISBAS) InSAR method to the South Wales Coalfield, UK. *International Journal of Applied Earth Observation and Geoinformation*, *34*(1), 249–257. https://doi.org/10.1016/j.jag.2014.08.018

Berardino, P., Fornaro, G., Lanari, R., & Sansosti, E. (2002). A new algorithm for surface deformation monitoring based on small baseline differential SAR interferograms. *IEEE Transactions on Geoscience and Remote Sensing*, *40*(11), 2375–2383. https://doi.org/10.1109/TGRS.2002.803792

BNPB. (2018). Indonesia Disaster Infographics in December 2018. Retrieved from https://bnpb.go.id/uploads/24/info-bencana-desember-2018.pdf. [July 17, 2021]

BNPB. (2019). Indonesia Disaster Infographics in 2019. Retrieved from https://bnpb.go.id/infografis. [July 17, 2021]

BNPB. (2021). Indonesia Disaster Infographics in 2021. Retrieved from https://bnpb.go.id/infografis. [July 17, 2021]

Bobrowsky, P., & Highland, L. (2013). The Landslide Handbook- A Guide to Understanding Landslides: A landmark publication for landslide education and preparedness. In *Landslides: Global Risk Preparedness*. https://doi.org/10.1007/978-3-642-22087-6_5

Bogaard, T., & Greco, R. (2018). Invited perspectives: Hydrological perspectives on precipitation intensity-duration thresholds for landslide initiation: Proposing hydro-meteorological thresholds. *Natural Hazards and Earth System Sciences*, *18*(1), 31–39. https://doi.org/10.5194/nhess-18-31-2018

Castellazzi, P., & Schmid, W. (2021). Interpreting C-band InSAR ground deformation data for large-scale groundwater management in Australia. *Journal of Hydrology: Regional Studies*, *34*(December 2020), 100774. https://doi.org/10.1016/j.ejrh.2021.100774

Casu, F., Manzo, M., & Lanari, R. (2006). A quantitative assessment of the SBAS algorithm performance for surface deformation retrieval from DInSAR data. *Remote Sensing of Environment*, *102*(3–4), 195–210. https://doi.org/10.1016/j.rse.2006.01.023

Çellek, S. (2020). Effect of the Slope Angle and Its Classification on Landslide. *Natural Hazards and Earth System Sciences*, *May*, 1–23. https://doi.org/10.5194/nhess-2020-87

Cianflone, G., Tolomei, C., Brunori, C. A., Monna, S., & Dominici, R. (2018). Landslides and subsidence assessment in the Crati Valley (Southern Italy) using InSAR data. *Geosciences (Switzerland)*, *8*(2). https://doi.org/10.3390/geosciences8020067

Cigna, F., & Sowter, A. (2017). The relationship between intermittent coherence and precision of ISBAS InSAR ground motion velocities: ERS-1/2 case studies in the UK. *Remote Sensing of Environment*, *202*, 177–198. https://doi.org/10.1016/j.rse.2017.05.016

Cogan, J., & Gratchev, I. (2019). A study on the effect of rainfall and slope characteristics on landslide initiation using flume tests. *Landslides*, *16*(12), 2369–2379. https://doi.org/10.1007/s10346-019-01261-0

Crosetto, M., Copons, R., Cuevas-González, M., Devanthéry, N., & Monserrat, O. (2018). Monitoring soil creeps landslides in an urban area using persistent scatterer interferometry (El Papiol, Catalonia, Spain). *Landslides*, *15*(7), 1317–1329. https://doi.org/10.1007/s10346-018-0965-5

Damayanti, A., Angin, F., Adib, A., & Irfan, M. (2020). Geomorphological Characteristic of Landslide Hazard Zones in Sukarame Village, Cisolok Subdistrict, Sukabumi Regency. *IOP Conference Series: Earth and Environmental Science*, *412*(1). https://doi.org/10.1088/1755-1315/412/1/012009

De Luca, C., Bonano, M., Casu, F., Manunta, M., Manzo, M., Onorato, G., Zinno, I., & Lanari, R. (2018). The parallel SBAS-DINSAR processing chain for the generation of national scale sentinel-1 deformation time-series. *Procedia Computer Science*, *138*, 326–331. https://doi.org/10.1016/j.procs.2018.10.046

Dehghani, M., & Javadi, H. R. (2013). Remote sensing of ground deformation. *SPIE Newsroom*, *November*, 2–5. https://doi.org/10.1117/2.1201303.004772

El Jazouli, A., Barakat, A., & Khellouk, R. (2020). Geotechnical studies for Landslide susceptibility in the high basin of the Oum Er Rbia river (Morocco). *Geology, Ecology, and Landscapes*, *00*(00), 1–8. https://doi.org/10.1080/24749508.2020.1743527

Guo, J., Yi, S., Yin, Y., Cui, Y., Qin, M., Li, T., & Wang, C. (2020). The effect of topography on landslide kinematics: a case study of the Jichang town landslide in Guizhou, China. *Landslides*, *17*(4), 959–973. https://doi.org/10.1007/s10346-019-01339-9

Hearn, G., Howell, J., & Hunt, T. (2020). Performance of slope stabilization trials on the road network of Laos. *Quarterly Journal of Engineering Geology and Hydrogeology*, *54*(1), 2021. https://doi.org/10.1144/qjegh2020-064

Lanari, R., Casu, F., Manzo, M., & Lundgren, P. (2007). Application of the SBAS-DInSAR technique to fault creep A case study of the Hayward fault, California. *Remote Sensing of Environment*, *109*(1), 20–28. https://doi.org/10.1016/j.rse.2006.12.003

Li, L., Yao, X., Yao, J., Zhou, Z., Feng, X., & Liu, X. (2019). Analysis of deformation characteristics for a reservoir landslide before and after impoundment by multiple D-InSAR observations at Jinshajiang River, China. *Natural Hazards*, *98*(2), 719–733. https://doi.org/10.1007/s11069-019-03726-w

Malinowska, A. A., Witkowski, W. T., Guzy, A., & Hejmanowski, R. (2020). Satellite-based monitoring and modeling of ground movements caused by water rebound. *Remote Sensing*, *12*(11). https://doi.org/10.3390/rs12111786

Martins, B. H., Suzuki, M., Yastika, P. E., & Shimizu, N. (2020). Ground surface deformation detection in complex landslide area—bobonaro, Timor-Leste—using SBAS DinSAR, UAV photogrammetry, and field observations. *Geosciences (Switzerland)*, *10*(6), 1–26. https://doi.org/10.3390/geosciences10060245

Morishita, Y., Lazecky, M., Wright, T. J., Weiss, J. R., Elliott, J. R., & Hooper, A. (2020). LiCSBAS: An open-source InSAR time series analysis package integrated with the LiCSAR automated sentinel-1 InSAR processor. *Remote Sensing*, *12*(3), 5–8. https://doi.org/10.3390/rs12030424

Ng, A. H. M., Ge, L., Li, X., Abidin, H. Z., Andreas, H., & Zhang, K. (2012). Mapping land subsidence in Jakarta, Indonesia using persistent scatterer interferometry (PSI) technique with ALOS PALSAR. *International Journal of Applied Earth Observation and Geoinformation*, *18*(1), 232–242. https://doi.org/10.1016/j.jag.2012.01.018

North, M., Farewell, T., Hallett, S., & Bertelle, A. (2017). Monitoring the response of roads and railways to seasonal soil movement with persistent scatterers interferometry over six UK sites. *Remote Sensing*, *9*(9). https://doi.org/10.3390/rs9090922

Novellino, A., Cigna, F., Sowter, A., Ramondini, M., & Calcaterra, D. (2017). Exploitation of the Intermittent SBAS (ISBAS) algorithm with COSMO-SkyMed data for landslide inventory mapping in north-western Sicily, Italy. *Geomorphology*, *280*, 153–166. https://doi.org/10.1016/j.geomorph.2016.12.009

Nowicki Jessee, M. A., Hamburger, M. W., Ferrara, M. R., McLean, A., & FitzGerald, C. (2020). A global dataset and model of earthquake-induced landslide fatalities. *Landslides*, *17*(6), 1363–1376. https://doi.org/10.1007/s10346-020-01356-z

Pawlik, Ł., & Šamonil, P. (2018). Soil creep The driving factors, evidence, and significance for bio-geomorphic and pedogenic domains and systems – A critical literature review. *Earth-Science Reviews*, *178*(January), 257–278. https://doi.org/10.1016/j.earscirev.2018.01.008

Pawluszek-Filipiak, K., & Borkowski, A. (2020). Integration of DInSAR and SBAS techniques to determine mining-related deformations using Sentinel-1 data: The case study of rydultowy mine in Poland. *Remote Sensing*, *12*(2). https://doi.org/10.3390/rs12020242

Pepe, A., & Calò, F. (2017). A review of interferometric synthetic aperture RADAR (InSAR) multi-track approaches for retrieving Earth's Surface displacements. *Applied Sciences (Switzerland)*, *7*(12). https://doi.org/10.3390/app7121264

Perera, E. N. C., Jayawardana, D. T., Jayasinghe, P., Bandara, R. M. S., & Alahakoon, N. (2018). Direct impacts of landslides on socio-economic systems: a case study from Aranayake, Sri Lanka. *Geoenvironmental Disasters*, *5*(1). https://doi.org/10.1186/s40677-018-0104-6

Persichillo, M. G., Bordoni, M., & Meisina, C. (2017). The role of land-use changes in the distribution of shallow landslides. *Science of the Total Environment*, *574*, 924–937. https://doi.org/10.1016/j.scitotenv.2016.09.125

Prasetyo, Y., Firdaus, H. S., & Diyanah. (2019). Land Subsidence of Semarang City Using Permanent Scatterer Interferometric Synthetic Aperture Radar (Ps-Insar) Method in Sentinel 1a between 2014-2017. *IOP Conference Series: Earth and Environmental Science*, *313*(1). https://doi.org/10.1088/1755-1315/313/1/012044

Qu, T., Lu, P., Liu, C., & Wan, H. (2016). Application of time series InSAR technique for deformation monitoring of large-scale landslides in mountainous areas of western China. *International Archives of the Photogrammetry, Remote Sensing and Spatial Information Sciences - ISPRS Archives*, *2016-Janua*(July), 89–91. https://doi.org/10.5194/isprsarchives-XLI-B1-89-2016

Ramirez, R., Lee, S. R., & Kwon, T. H. (2020). Long-term remote monitoring of ground deformation using sentinel-1 interferometric synthetic aperture radar (InSAR): Applications and insights into geotechnical engineering practices. *Applied Sciences (Switzerland)*, *10*(21), 1–20. https://doi.org/10.3390/app10217447

Remy, D., Bonvalot, S., Briole, P., & Murakami, M. (2003). Accurate measurements of tropospheric effects in volcanic areas from SAR interferometry data: Application to Sakurajima volcano (Japan). *Earth and Planetary Science Letters*, *213*(3–4), 299–310. https://doi.org/10.1016/S0012-821X(03)00331-5

Ristya, Y., Supriatna, & Sobirin. (2019). Spatial pattern of potential landslide area by SMORPH, INDEX STORIE, and SINMAP method in Pelabuhanratu and surrounding area, Indonesia. *IOP Conference Series: Earth and Environmental Science*, *338*(1). https://doi.org/10.1088/1755-1315/338/1/012033

Roccheggiani, M., Piacentini, D., Tirincanti, E., Perissin, D., & Menichetti, M. (2019). Detection and monitoring of tunneling induced ground movements using Sentinel-1 SAR interferometry. *Remote Sensing*, *11*(6). https://doi.org/10.3390/rs11060639

Shirani, K., & Pasandi, M. (2019). Detecting and monitoring of landslides using persistent scattering synthetic aperture radar interferometry. *Environmental Earth Sciences*, *78*(1), 1–24. https://doi.org/10.1007/s12665-018-8042-x

Skrzypczak, I., Kokoszka, W., Zientek, D., Tang, Y., & Kogut, J. (2021). Landslide hazard assessment map as an element supporting spatial planning: The flysch Carpathians region study. *Remote Sensing*, *13*(2), 1–20. https://doi.org/10.3390/rs13020317

Sugianti, K., Sukristiyanti, S., & Tohari, A. (2016). Model Kerentanan Gerakan Tanah Wilayah Kabupaten Sukabumi Secara Spasial Dan Temporal. *Jurnal RISET Geologi Dan Pertambangan*, *26*(2), 117. https://doi.org/10.14203/risetgeotam2016.v26.270

Virk, A. S., Singh, A., & Mittal, S. K. (2019). Monitoring and analysis of displacement using InSAR techniques for Gulaba landslide site. *Journal of Engineering Science and Technology*, *14*(3), 1558–1571.

Wasowski, J., & Bovenga, F. (2014). Investigating landslides and unstable slopes with satellite Multi-Temporal Interferometry: Current issues and future perspectives. *Engineering Geology*, *174*, 103–138. https://doi.org/10.1016/j.enggeo.2014.03.003

Yastika, P. E., Shimizu, N., & Abidin, H. Z. (2019). Monitoring long-term land subsidence from 2003 to 2017 in the coastal area of Semarang, Indonesia by SBAS DInSAR analyses using Envisat-ASAR, ALOS-PALSAR, and Sentinel-1A SAR data. *Advances in Space Research*, *63*(5), 1719–1736. https://doi.org/10.1016/j.asr.2018.11.008

Zaenudin, A., Darmawan, I. G. B., Armijon, Minardi, S., & Haerudin, N. (2018). Land subsidence analysis in Bandar Lampung City based on InSAR. *Journal of Physics: Conference Series*, *1080*(1). https://doi.org/10.1088/1742-6596/1080/1/012043

Zollini, S., Alicandro, M., Cuevas-González, M., Baiocchi, V., Dominici, D., & Buscema, P. M. (2020). Shoreline extraction based on an active connection matrix (ACM) image enhancement strategy. *Journal of Marine Science and Engineering*, *8*(1). https://doi.org/10.3390/jmse8010009

Zuidam, R. A. van. (1985). Aerial photo interpretation in terrain analysis and geomorphologic mapping. In *Aerial photo interpretation in terrain analysis and geomorphologic mapping*. Smits.